ФИЗИКА ЭЛЕМЕНТАРНЫХ ЧАСТИЦ И АТОМНОГО ЯДРА. ТЕОРИЯ

COULOMB CORRECTIONS
TO THE PARAMETERS OF THE
LANDAU–POMERANCHUK–MIGDAL EFFECT THEORY

O. O. Voskresenskaya, E. A. Kuraev, H. T. Torosyan

Joint Institute for Nuclear Research, Dubna

Using the Coulomb correction to the screening angular parameter of the Molière multiple scattering theory, we obtained analytically and numerically the Coulomb corrections to the quantities of the Migdal LPM-effect theory. We showed that the Coulomb correction to the spectral bremsstrahlung rate allows completely eliminating the discrepancy between the predictions of the LPM effect theory and its measurement at least for high-Z targets and also to further improve the agreement between the predictions of the LPM effect theory analogue for a thin layer of matter and experimental data.

С использованием кулоновской поправки к углу экранирования теории многократного рассеяния Мольера аналитически и численно найдены кулоновские поправки для ряда параметров мигдаловской теории ЛПМ-эффекта. Показано, что полученная кулоновская поправка для спектральной плотности излучения электронов позволяет полностью преодолеть расхождение между предсказаниями теории ЛПМ-эффекта и результатами его измерения для мишеней из тяжелых элементов, а также улучшить соответствие между предсказаниями аналога теории ЛПМ-эффекта для тонкой мишени и экспериментальными данными.

INTRODUCTION

Landau and Pomeranchuk were the first to show [1] that multiplicity of electron scattering processes by atomic nuclei in an amorphous medium results in the suppression of soft bremsstrahlung. The quantitative theory of this phenomenon was created by Migdal [2, 3][1]. Therefore, it received the name Landau–Pomeranchuk–Migdal (LPM) effect.

The next step in the development of the quantitative theory of the LPM effect was made in [5] on the basis of the quasi-classical operator method in QCD [6]. One of the basic equations of this method is the Schrödinger equation in the external field with an imaginary potential, which admits of formal solution in the form of the path integral. The path integral treatment of the LPM effect was proposed and developed in [7–12].

It was shown that analogous effects are also possible at coherent radiation of relativistic electrons and positrons in a crystalline medium [13], in cosmic-ray physics [14] (e.g., in applications motivated by extremely high-energy IceCubes neutrino-induced showers with energies above 1 PeV [15]). Effects of this kind should manifest themselves in scattering of protons

---

[1]See also [4] accounting for the edge effects.

by the nuclei, which has recently been shown in Groning by the AGOR collaboration [16], and penetration of quarks through the nuclear matter at the RHIC and LHC energies [17]. The QCD analogue of the LPM effect was examined in [8, 18, 19]; a possibility studying the LPM effect in oriented crystal at GeV energy was analyzed in [20]; theoretically, an analogue of the LPM effect was considered for nucleon–nucleon collisions in the neutron stars, supernovae [21], and relativistic plasmas [22].

The results of a series of experiments at the SLAC [23–25] and CERN-SPS [26, 27] accelerators on detection of the Landau–Pomeranchuk effect confirmed the basic qualitative conclusion that multiple scattering of ultrarelativistic charged particles in matter leads to suppression of their bremsstrahlung in the soft part of the spectrum. However, attempts to quantitatively describe the experimental data [23] faced an unexpected difficulty. For achieving satisfactory agreement of data with theory [2,3], the authors [23] had to multiply the results of their calculations in the Born approximation by the normalization factor R equal to $0.94 \pm 0.01 \pm 0.032$, which had no reasonable explanation.

The alternate calculations [9, 11] gave a similar result despite different computational basis [23]. The theoretical predictions are in agreement with the spectrum of photon bremsstrahlung measured for 25 GeV electron beam and $0.7-6.0\% L_R$[1] gold target over the range $30 < \omega < 500$ MeV of the emitted photon frequency ω only within a normalization factor 0.93 [9] – 0.94 [23]. The origin of the above small but significant disagreement between data and theory needs to be better understood [24]. In [10] the further development of the light-cone path integral approach to PLM effect was performed. The Coulomb effects, as well as multiphoton emission and absorbtion, was taken into account. A detailed comparison with SLAC E-146 data was carried out. Nevertheless, the problem of normalization remained and is still not clear. The other authors, except those of [9,10], do not discuss normalization [25].

The aim of this work is to show that the discussed discrepancy between data and theory can be explained at least for high-Z targets if the corrections to the results of the Born approximation (i.e., the so-called Coulomb corrections) are appropriately considered on the basis of a revised version of the Molière multiple scattering theory [28,29].

The paper is organized as follows. In Sec. 1 we consider the basic formulae of the quantitative LPM effect theory for finite-size targets obtained by the kinetic equation method and also the small-angle approximation of this theory which is further used for analytical and numerical calculations. In Sec. 2 we present the results of the conventional [30] and a revised small-angle Molière multiple scattering theory [28, 29] applied in the next section to the theory of the LPM effect and its analogue for a thin target [32, 33]. In Sec. 3 we obtain the analytical and numerical results for Coulomb corrections to the quantities of the LPM effect theory and its analogue for a thin layer of matter in some asymptotic cases and also in the regimes corresponding to the conditions of the experiment [28, 29]. Finally, in Sec. 4 we summarize our findings and state our conclusions.

1. LPM EFFECT THEORY FOR FINITE TARGETS

There exist two methods that allow one to develop a rigorous quantitative theory of the Landau–Pomeranchuk effect. This is Migdal's method of kinetic equation [2, 3] and

---

[1]L_R presents a radiation length of a target material here.

the method of functional integration [7–12, 31]. Neglecting numerically small quantum-mechanical corrections, we will adhere to version of the Landau–Pomeranchuk effect theory, developed in [2, 4, 35].

1.1. Basic Formulae. Simple though quite cumbersome calculations using the results [2, 4] yield the following formula for the electron spectral bremsstrahlung intensity averaged over various trajectories of electron motion in an amorphous medium (hereafter the units $\hbar = c = 1$, $e^2 = 1/137$ are used) [35]:

$$\left\langle \frac{dI}{d\omega} \right\rangle = 2 \sum_{\epsilon} \left\{ n_0 L \int f^*(\mathbf{n}_2)\, \nu(\mathbf{n}_2 - \mathbf{n}_1) f(\mathbf{n}_1)\, d\mathbf{n}_1\, d\mathbf{n}_2 - \right.$$

$$- (n_0 v)^2 \int\limits_0^T dt_1 \int\limits_{t_1}^T dt_2\, \mathrm{Re}\left[\int f^*(\mathbf{n}_2)\nu(\mathbf{n}_2 - \mathbf{n}_2')f(\mathbf{n}_1) \times \right.$$

$$\left. \left. \times\, \nu(\mathbf{n}_1' - \mathbf{n}_1) w(t_2, t_1, \mathbf{n}_2', \mathbf{n}_1', \mathbf{k})\, d\mathbf{n}_1\, d\mathbf{n}_1'\, d\mathbf{n}_2\, d\mathbf{n}_2' \right] \right\}, \quad (1)$$

where

$$f(\mathbf{n}_{1,2}) = \frac{e}{2\pi} \frac{\boldsymbol{\epsilon}\mathbf{v}_{1,2}}{1 - \mathbf{n} \cdot \mathbf{v}_{1,2}},$$

$$\mathbf{v}_{1,2} = v \cdot \mathbf{n}_{1,2}, \quad \mathbf{n} = \frac{\mathbf{k}}{\omega}, \quad d\mathbf{n}_{1,2} \equiv do_{1,2}, \quad T = \frac{L}{v},$$

$$\nu(\mathbf{n}_2 - \mathbf{n}_1) = \delta(\mathbf{n}_2 - \mathbf{n}_1) \int \sigma_0(\mathbf{n}_2' - \mathbf{n}_1)\, d\mathbf{n}_2' - \sigma_0(\mathbf{n}_2 - \mathbf{n}_1),$$

$$w(t_2, t_1, \mathbf{n}_2, \mathbf{n}_1, \mathbf{k}) = \int \widetilde{w}(t_2, t_1, \mathbf{r}_2 - \mathbf{r}_1, \mathbf{n}_2, \mathbf{n}_1) \exp\left[i\omega(t_2 - t_1) - i\mathbf{k}(\mathbf{r}_2 - \mathbf{r}_1)\right] d\mathbf{r}_2.$$

Here $\boldsymbol{\epsilon}$ and $\mathbf{k}$ are the polarization vector and the wave vector of the emitted photon; n_0 denotes the density of the scattering centers per unit length of fast scattered particle trajectory; L is the target thickness; $\mathbf{n}_{1,2}$ are the unit vectors in the electron motion direction; $\mathbf{v}$ and v are the electron velocity assumed to be invariant during the interaction with the target (the quantum-mechanical recoil effect is negligibly small) and its modulus; e is the electron charge; $\sigma_0(\mathbf{n}_2 - \mathbf{n}_1) = d\sigma/do_{\mathbf{n}_2}$ presents the differential Born cross section of the electron scattering by target atoms. The direction of motion $\mathbf{n}_2$ at time t_2 provided that at the time t_1 the electron had the coordinate $\mathbf{r}_1$ and moved in the direction characterized by the unit vector $\mathbf{n}_1$. The electron distribution function in the coordinate $\mathbf{r}_2$, $w(t_2, t_1, \mathbf{r}_2 - \mathbf{r}_1, \mathbf{n}_2, \mathbf{n}_1)$, satisfies the kinetic equation

$$\frac{\partial w(t_2, t_1, \mathbf{r}_2 - \mathbf{r}_1, \mathbf{n}_2, \mathbf{n}_1)}{\partial t_2} = -\mathbf{v}_2 \cdot \boldsymbol{\nabla}_{\mathbf{r}_2} w(t_2, t_1, \mathbf{r}_2 - \mathbf{r}_1, \mathbf{n}_2, \mathbf{n}_1) -$$

$$- n_0 \int \nu(\mathbf{n}_2 - \mathbf{n}_1') \widetilde{w}(t_2, t_1, \mathbf{r}_2 - \mathbf{r}_1, \mathbf{n}_2', \mathbf{n}_1)\, d\mathbf{n}_2' \quad (2)$$

with the boundary condition

$$\widetilde{w}(t_2, t_1, \mathbf{r}_2 - \mathbf{r}_1, \mathbf{n}_2, \mathbf{n}_1)|_{t_2 = t_1} = \delta(\mathbf{r}_2 - \mathbf{r}_1)\, \delta(\mathbf{n}_2 - \mathbf{n}_1). \quad (3)$$

The term of (1) linear in n_0 is a «usual» (incoherent) contribution to the intensity of the electron bremsstrahlung in the medium, derived by summation of the radiation intensities of the electron interaction with separate atoms of the target. The term quadratic in n_0 includes the contribution from the interference of the bremsstrahlung amplitudes on various atoms. The destructive character of this interference leads to suppression of the soft radiation intensity, i.e., to the Landau–Pomeranchuk effect.

For ω larger than $\omega_{\mathrm{cr}} = 4\pi\gamma^2/(e^2 L_R)$, where γ is the Lorentz factor of the scattered particle and L_R is the radiation length of the target material (for estimation of ω_{cr}, see [1, 2, 10, 32])[1], the interference term becomes negligibly small, and radiation is of pure incoherent character.

1.2. Small-Angle Approximation. For ultrarelativistic particles $(1-v \ll 1)$ it is convenient to pass in (1) to the small-angle approximation $(\vartheta_{1,2} \ll 1)$ according to the scheme

$$\mathbf{n}_{1,2} = \left(1 - \frac{\vartheta_{1,2}^2}{2}\right)\mathbf{n} + \boldsymbol{\vartheta}_{1,2}, \quad d\mathbf{n}_{1,2} = d\boldsymbol{\vartheta}_{1,2};$$

$$f(\mathbf{n}_{1,2}) = f(\boldsymbol{\vartheta}_{1,2}) = \frac{e}{\pi}\frac{\boldsymbol{\epsilon}\,\boldsymbol{\vartheta}_{1,2}}{\vartheta_{1,2}^2 + \lambda^2}, \quad \lambda = \frac{m}{E} = \gamma^{-1};$$

$$\sigma_0(\mathbf{n}_2 - \mathbf{n}_1) = \sigma_0(\boldsymbol{\vartheta}_2 - \boldsymbol{\vartheta}_1), \quad \delta(\mathbf{n}_2 - \mathbf{n}_1) = \delta(\boldsymbol{\vartheta}_2 - \boldsymbol{\vartheta}_1), \tag{4}$$

$$\nu(\mathbf{n}_2 - \mathbf{n}_1) = \nu(\boldsymbol{\vartheta}_2 - \boldsymbol{\vartheta}_1), \quad \boldsymbol{\vartheta}_2 - \boldsymbol{\vartheta}_1 = \boldsymbol{\theta};$$

$$w(t_2, t_1, \mathbf{n}_2, \mathbf{n}_1, \mathbf{k}) = w(t_2, t_1, \boldsymbol{\vartheta}_2, \boldsymbol{\vartheta}_1, \omega)$$

and further to the Fourier transforms of f, ν, w:

$$f(\boldsymbol{\eta}) = \frac{1}{2\pi}\int \widetilde{f}(\boldsymbol{\theta})\exp\left[i\boldsymbol{\eta}\boldsymbol{\theta}\right]d\boldsymbol{\theta} = \frac{ie\lambda\boldsymbol{\epsilon}\,\boldsymbol{\eta}}{\pi\eta}K_1(\lambda\eta),$$

$$\nu(\eta) = \int \widetilde{\nu}(\boldsymbol{\theta})\,e^{i\boldsymbol{\eta}\boldsymbol{\theta}}\,d\boldsymbol{\theta} = 2\pi\int \sigma_0(\boldsymbol{\theta})[1 - J_0(\eta\theta)]\boldsymbol{\theta}\,d\boldsymbol{\theta}, \tag{5}$$

$$w(t_2, t_1, \boldsymbol{\eta}_2, \boldsymbol{\eta}_1, \omega) = \frac{1}{(2\pi)^2}\int \widetilde{w}(t_2, t_1, \boldsymbol{\vartheta}_2, \boldsymbol{\vartheta}_1, \omega)\exp\left[i\boldsymbol{\eta}_2\boldsymbol{\vartheta}_2 - i\boldsymbol{\eta}_1\boldsymbol{\vartheta}_1\right]d\boldsymbol{\vartheta}_1\,d\boldsymbol{\vartheta}_2,$$

where $\boldsymbol{\vartheta}_{1(2)}$ denotes a two-dimensional electron scattering angle in the plane orthogonal to the electron direction at instant of time $t_{1(2)}$; m and E are the electron mass and its energy; $\boldsymbol{\theta}$ presents the electron scattering angle over the time interval $t_2 - t_1$; λ is the characteristic frequency of the emitted photon; J_0 and K_1 are the Bessel and Macdonald functions, respectively.

Consequently, expression (1) is reduced to

$$\left\langle \frac{dI}{d\omega} \right\rangle = \frac{2\lambda^2 e^2}{\pi^2}\left\{ n_0 L \int K_1^2(\lambda\eta)\nu(\eta)\,d\boldsymbol{\eta} - \right.$$

$$- n_0^2\int_0^L dt_1 \int_0^L dt_2 \int \frac{(\boldsymbol{\eta}_1\boldsymbol{\eta}_2)}{\eta_1\eta_2}K_1(\lambda\eta_1)\,K_1(\lambda\eta_2)\,\nu(\eta_1)\,\nu(\eta_2)\times$$

$$\left. \times \mathrm{Re}\left[w(t_2, t_1, \boldsymbol{\eta}_2, \boldsymbol{\eta}_1, \omega)\right]d\boldsymbol{\eta}_1\,d\boldsymbol{\eta}_2 \right\}, \tag{6}$$

---

[1]In the conditions of experiment [23, 24], $\omega_{\mathrm{cr}} \approx 244$ MeV for $0.7 - 6.0\%L_R$ gold target at 25 GeV (see Table 1 in [10]).

where w satisfies the kinetic equation

$$\frac{\partial w(t_2, t_1, \boldsymbol{\eta}_2, \boldsymbol{\eta}_1, \omega)}{\partial t_2} = \frac{i\omega}{2}(\lambda^2 - \Delta_{\boldsymbol{\eta}_2})w(t_2, t_1, \boldsymbol{\eta}_2, \boldsymbol{\eta}_1, \omega) - n_0\nu(\eta_2)\, w(t_2, t_1, \boldsymbol{\eta}_2, \boldsymbol{\eta}_1, \omega) \quad (7)$$

or, equivalently,

$$i\,\frac{\partial w(t_2, t_1, \boldsymbol{\eta}_2, \boldsymbol{\eta}_1, \omega)}{\partial t_2} = \left[\frac{\omega}{2}\Delta_{\boldsymbol{\eta}_2} - \frac{\omega}{2}\lambda^2 - in_0\nu(\eta_2)\right] w(t_2, t_1, \boldsymbol{\eta}_2, \boldsymbol{\eta}_1, \omega) \quad (8)$$

with the boundary condition

$$w(t_2, t_1, \boldsymbol{\eta}_2, \boldsymbol{\eta}_1, \omega) = \delta(\boldsymbol{\eta}_2 - \boldsymbol{\eta}_1). \quad (9)$$

The form of (8) is similar to the equation for Green's function of the two-dimensional Schrödinger equation with the mass ω^{-1} and the complex potential

$$U(\eta) = -\frac{\omega\lambda^2}{2} - i\,n_0\nu(\eta) \quad (10)$$

and therefore admits of a formal solution in the form of a continual integral (see, e.g., [34]). The analysis of (6) will be continued in Sec. 3.

2. MULTIPLE SCATTERING THEORY

The theory of the multiple scattering of charged particles has been treated by several authors. However, most widespread at present is the multiple scattering theory of Molière [30, 31]. The results of this theory are employed nowadays in most of the transport codes. It is of interest for numerous applications related to particle transport in matter and also presents the most used tool for taking into account the multiple scattering effects in experimental data processing.

As the Molière theory is currently used roughly for $10-300$ GeV electron beams, the role of the high-energy corrections to the parameters of this theory becomes significant. Of special importance is the Coulomb correction to the screening angular parameter, as this parameter also enters into other important quantities in the Molière theory.

2.1. Molière's Theory of Multiple Scattering. Let $w_M(\boldsymbol{\vartheta}, L)$ be a spatial-angle particle distribution function in a homogenous medium, $\boldsymbol{\vartheta} = (\vartheta, \varphi)$ is a two-dimensional particle scattering angle in the plane orthogonal to the incident particle direction and L is the target thickness. Owing to the axial symmetry of the above distribution function in most cases of interest, it is independent of the azimuthal angle φ, and in the notation of Molière it reads

$$w_M(\vartheta, L) = \int\limits_0^\infty J_0(\vartheta\eta) \exp\left[-n_0 L\,\nu(\eta)\right]\eta\, d\eta, \quad (11)$$

where

$$\nu(\eta) = 2\pi \int\limits_0^\infty \sigma_0(\boldsymbol{\theta})[1 - J_0(\theta\eta)]\boldsymbol{\theta}\, d\boldsymbol{\theta}. \quad (12)$$

The function (11) satisfies the well-known Boltzmann transport equation, written here with the small-angle approximation $\vartheta \ll 1$ $(\sin\vartheta \sim \vartheta)$

$$\frac{\partial w(\vartheta, L)}{\partial L} = -n_0 w_M(\vartheta, L) \int \sigma_0(\boldsymbol{\theta})\, d^2\boldsymbol{\theta} + n_0 \int w_M(\boldsymbol{\vartheta} + \boldsymbol{\theta}, L)\, \sigma_0(\boldsymbol{\theta})\, d^2\boldsymbol{\theta} =$$

$$= n_0 \int \left[w_M(\boldsymbol{\vartheta} + \boldsymbol{\theta}, L) - w_M(\vartheta, L) \right] \sigma_0(\boldsymbol{\theta})\, d^2\boldsymbol{\theta}. \quad (13)$$

The Gaussian particle distribution function used in the Migdal LPM effect theory, which differs from (11), can be derived from the Boltzmann transport equation by the method of Fokker and Planck [36].

One of the most important results of the Molière theory is that the scattering is described by a single parameter, the so-called screening angle $(\theta_a$ or $\theta_a')$

$$\theta_a' = \sqrt{1.167}\theta_a = \left[\exp\left(C_E - 0.5 \right) \right] \theta_a \approx 1.080\theta_a, \quad (14)$$

where $C_E = 0.577\ldots$ is the Euler constant.

More precisely, the angular distribution depends only on the logarithmic ratio b,

$$b = \ln\left(\frac{\theta_c}{\theta_a'} \right)^2 \equiv \ln\left(\frac{\theta_c}{\theta_a} \right)^2 + 1 - 2C_E, \quad (15)$$

of the characteristic angle θ_c describing the foil thickness

$$\theta_c^2 = 4\pi n_0 L \left(\frac{Z\alpha}{\beta p} \right)^2, \quad p = mv, \quad (16)$$

to the screening angle θ_a', which characterizes the scattering atom.

In order to obtain a result valid for large angles, Molière defines a new parameter B by the transcendental equation

$$B - \ln B = b. \quad (17)$$

The angular distribution function can then be written as

$$w_M(\vartheta, B) = \frac{1}{\vartheta^2} \int\limits_0^\infty y\, dy\, J_0(\vartheta y) e^{-y^2/4} \exp\left[\frac{y^2}{4B} \ln\left(\frac{y^2}{4} \right) \right], \quad y = \theta_c \eta. \quad (18)$$

The Molière expansion method is to consider the term $y^2 \ln\left(y^2/4 \right)/4B$ as a small parameter. Then, the angular distribution function is expanded in a power series in $1/B$:

$$w_M(\vartheta, L) = \sum_{n=0}^\infty \frac{1}{n!} \frac{1}{B^n} w_n(\vartheta, L), \quad (19)$$

in which

$$w_n(\vartheta, L) = \frac{1}{\overline{\vartheta^2}} \int\limits_0^\infty y\, dy\, J_0\left(\frac{\vartheta}{\sqrt{\overline{\vartheta^2}}} y \right) e^{-y^2/4} \left[\frac{y^2}{4} \ln\left(\frac{y^2}{4} \right) \right]^n, \quad (20)$$

$$\overline{\vartheta^2} = \theta_c^2 B = 4\pi n_0 L \left(\frac{Z\alpha}{\beta p} \right)^2 B(L). \quad (21)$$

This method is valid for $B \geqslant 4.5$ and $\overline{\vartheta^2} < 1$.

The first function $w_0(\vartheta, L)$ has a simple analytical form

$$w_0(\vartheta, L) = \frac{2}{\overline{\vartheta}^2} \exp\left(-\frac{\vartheta^2}{\overline{\vartheta}^2}\right), \tag{22}$$

$$\overline{\vartheta}^2 \underset{L \to \infty}{\sim} \frac{L}{L_R} \ln\left(\frac{L}{L_R}\right). \tag{23}$$

For small angles, i.e., $\vartheta/\overline{\vartheta} = \vartheta/(\theta_c\sqrt{B})$ less than about 2, the Gaussian (22) is the dominant term. In this region, $w_1(\vartheta, L)$ is in general less than $w_0(\vartheta, L)$, so that the correction to the Gaussian is of order of $1/B$, i.e., about 10%.

A good approximate representation of the distribution at any angle is

$$w_M(\vartheta, L) = w_0(\vartheta, L) + \frac{1}{B} w_1(\vartheta, L) \tag{24}$$

with

$$w_1(\vartheta, L) = \frac{1}{\overline{\vartheta}^2} \int\limits_0^\infty y\, dy\, J_0\left(\frac{\vartheta}{\sqrt{\overline{\vartheta}^2}} y\right) \mathrm{e}^{-y^2/4} \left[\frac{y^2}{4} \ln\left(\frac{y^2}{4}\right)\right]. \tag{25}$$

This approximation was applied by the authors of [33] to the analysis of data [23, 24] over the region $\omega < 30$ MeV that will be shown in Sec. 3.

Let us notice that the expression (12) for the function $\nu(\eta)$ is identical to (5). As was shown in classical works of Molière [30], this quantity can be represented in the area of the important η values $0 \leqslant \eta \leqslant 1/\theta_c$ as

$$\nu(\eta) = -4\pi \left(\frac{Z\alpha}{\beta p}\right)^2 \eta^2 \left[\ln\left(\frac{\eta\,\theta_a}{2}\right) + C_E - \frac{1}{2}\right], \tag{26}$$

where the screening angle θ_a depends both on the screening properties of the atom and on the $\sigma_0(\boldsymbol{\theta})$ approximation used for its calculation.

Using the Thomas–Fermi model of the atom and an interpolation scheme, Molière obtained θ_a for the cases where $\sigma_0(\boldsymbol{\theta})$ is calculated within the Born and quasi-classical approximations:

$$\theta_a^B = 1.20\alpha Z^{1/3}, \tag{27}$$

$$\theta_a = \theta_a^B \sqrt{1 + 3.34\left(\frac{Z\alpha}{\beta}\right)^2}. \tag{28}$$

The latter result is only approximate (see critical remarks on its derivation in [36]). Below we will present an exact analytical and numerical result for this angular parameter.

2.2. Coulomb Correction to the Screening Angular Parameter. Very recently, it has been shown [29] by means of [5] that for any model of the atom the following rigorous relation determining the screening angular parameter θ_a' is valid:

$$\ln\left(\theta_a'\right) = \ln\left(\theta_a'\right)^B + \mathrm{Re}\left[\psi\left(1 + \mathrm{i}\frac{Z\alpha}{\beta}\right)\right] + C_E$$

or, equivalently,

$$\Delta_{\mathrm{CC}}[\ln\left(\theta_a'\right)] \equiv \ln\left(\theta_a'\right) - \ln\left(\theta_a'\right)^B = f\left(\frac{Z\alpha}{\beta}\right), \tag{29}$$

where Δ_{CC} is the so-called Coulomb correction to the Born result, ψ is the logarithmic derivative of the gamma function Γ, and $f(Z\alpha/\beta)$ is a universal function of the Born parameter $\xi = Z\alpha/\beta$ which is also known as the Bethe–Maximon function:

$$f(\xi) = \xi^2 \sum_{n=1}^{\infty} \frac{1}{n(n^2 + \xi^2)}. \tag{30}$$

To compare the approximate Molière result (28) with the exact one (29), we first present (28) in the form

$$\delta_M \equiv \frac{\theta_a - \theta_a^B}{\theta_a^B} = \sqrt{1 + 3.34 \left(\frac{Z\alpha}{\beta}\right)^2} - 1 \tag{31}$$

and also rewrite (29) as follows:

$$\delta_{\mathrm{CC}} \equiv \frac{\theta_a - \theta_a^B}{\theta_a^B} = \frac{\theta_a' - \left(\theta_a'\right)^B}{\left(\theta_a'\right)^B} = \exp\left[f\left(\xi\right)\right] - 1. \tag{32}$$

Then we get

$$\delta_{\mathrm{MCC}} \equiv \frac{\delta_M - \delta_{\mathrm{CC}}}{\delta_M} = \frac{\Delta_{\mathrm{MCC}}}{\delta_M}. \tag{33}$$

For some high-Z targets used in [24] and $\beta = 1$, we have obtained the following values of relative Molière δ_M and Coulomb δ_{CC} corrections and also values of the difference Δ_{MCC} and relative difference δ_{MCC} between the approximate Molière (31) and exact (32) results (Table 1).

Table 1. **The difference between the approximate (31) and exact (32) results for the Coulomb correction to the screening angle in the range of nuclear charge** $74 < Z < 92$

Target	Z	$\delta_M, \%$	$\delta_{\mathrm{CC}}, \%$	$\Delta_{\mathrm{MCC}}, \%$	$\delta_{\mathrm{MCC}}, \%$
W	74	40.4	32.5	7.5	19.6
Pt	78	44.3	35.9	8.4	19.0
Au	79	45.2	36.7	8.5	18.8
Pb	82	48.2	39.3	8.9	18.5
U	92	58.3	48.5	9.8	16.9

For instance, Table 1 shows that the difference and relative difference between the approximate and exact results for these Coulomb corrections reach 8.5% and 18.8%, respectively, in the case of the gold target discussed in [9, 23, 24].

We show further that the aforesaid discrepancy between theory and experiment [9, 23, 24] can be completely eliminated for heavy-target elements on the basis of these Coulomb corrections to the screening angular parameter.

3. COULOMB CORRECTIONS IN THE LPM EFFECT THEORY AND ITS ANALOGUE FOR A THIN LAYER OF MATTER

3.1. Coulomb Corrections to the Parameters of the LPM Effect Theory for Finite Targets. Analytically solving Eq. (7) with arbitrary values of ω is only possible within the Fokker–Planck approximation[1]

$$\nu(\eta) = a\eta^2, \tag{34}$$

at $\omega = 0$ it is also possible for arbitrary $\nu(\eta)$.

In the latter case ($\omega = 0$)

$$w(t_2, t_1, \boldsymbol{\eta}_2, \boldsymbol{\eta}_1, 0) = \delta(\boldsymbol{\eta}_2 - \boldsymbol{\eta}_1) \exp\left[-n_0\nu(\eta_2)(t_2 - t_1)\right], \tag{35}$$

and integration over t_1, t_2 in (6) is carried out trivially, leading to the simple result

$$\left\langle \frac{dI}{d\omega} \right\rangle \bigg|_{\omega=0} = \frac{4\lambda^2 e^2}{\pi} \int K_1^2(\lambda\eta) \left\{1 - \exp\left[-n_0 L\nu(\eta)\right]\right\} \eta \, d\eta. \tag{36}$$

Considering the aforesaid, in the other limiting case ($\omega \gg \omega_{\mathrm{cr}}$) we get

$$\left\langle \frac{dI}{d\omega} \right\rangle \bigg|_{\omega \gg \omega_{\mathrm{cr}}} = n_0 L\lambda^2 e^2 \int K_1^2(\lambda\eta) \, \nu(\eta)\eta \, d\eta. \tag{37}$$

3.1.1. Case $\omega \gg \omega_{\mathrm{cr}}$. After the substitution of $\nu(\eta)$ (26) into (37), the integration is carried out analytically, leading to the following result:

$$\left\langle \frac{dI}{d\omega} \right\rangle \bigg|_{\omega \gg \omega_{\mathrm{cr}}} = \frac{16}{3\pi} \frac{Z^2 \alpha^3}{m^2} \left(\ln \frac{\lambda}{\theta_a} + \frac{7}{12}\right) n_0 L. \tag{38}$$

Let us find an analytical expression for the Coulomb correction to the Born spectral bremsstrahlung rate (38):

$$\Delta_{\mathrm{CC}}\left[\left\langle \frac{dI}{d\omega} \right\rangle\right] \equiv \left\langle \frac{dI}{d\omega} \right\rangle - \left\langle \frac{dI}{d\omega} \right\rangle^B =$$
$$= -\frac{16Z^2\alpha^3 n_0 L}{3\pi m^2} \left[\ln\left(\theta_a'\right) - \ln\left(\theta_a'\right)^B\right] = -\frac{16Z^2\alpha^3 n_0 L}{3\pi m^2} f(\xi). \tag{39}$$

Then, the corresponding relative Coulomb correction reads

$$\delta_{\mathrm{CC}}\left[\left\langle \frac{dI}{d\omega} \right\rangle\right] \equiv \frac{\langle dI/d\omega \rangle - \langle dI/d\omega \rangle^B}{\langle dI/d\omega \rangle^B} = -\frac{f(\xi)}{0.583 - \ln\left(1.2\alpha Z^{1/3}\right)}. \tag{40}$$

Let us enter the ratio

$$R_{\mathrm{CC}}(\omega) = \frac{\langle dI(\omega)/d\omega \rangle}{\langle dI(\omega)/d\omega \rangle^B} = \delta_{\mathrm{CC}}\left[\left\langle \frac{dI}{d\omega} \right\rangle\right] + 1. \tag{41}$$

We will now estimate the numerical values of (40) and (41) (Table 2).

---

[1] An explicit expression for w obtained in this approach can be found in [4].

Table 2. **The relative Coulomb correction** $\delta_{\mathrm{CC}}\left[\langle dI/d\omega\rangle\right]$ **to the Born spectral bremsstrahlung rate for some high-**Z **targets,** $\omega \gg \omega_{\mathrm{cr}}$**, and** $\beta = 1$

Target	Z	$Z\alpha$	$f(Z\alpha)$	$-\delta_{\mathrm{CC}}$	R_{CC}
W	74	0.540	0.281	0.072	0.928
Au	79	0.577	0.313	0.081	0.919
Pb	82	0.598	0.332	0.086	0.914
Note. $\bar{\delta}_{\mathrm{CC}}\left[\langle dI/d\omega\rangle\right] = (-7.97 \pm 0.71)\%$.					

It is seen from Table 2 that the relative correction to the Born spectral bremsstrahlung rate is about -8%, whereas the calculations of Blancenbekler and Drell [11] reproduce the Migdal results for thick targets with the $+8\%$ higher emission probability when the interference term vanishes. Therefore, it is natural to normalize these calculations by means of the obtained Coulomb correction $\bar{\delta}_{\mathrm{CC}}\left[\langle dI/d\omega\rangle\right] = (-7.97 \pm 0.71)\%$.

The corresponding ratio $R(\omega)|_{\omega \gg \omega_{\mathrm{cr}}}$ is approximately 0.92 for the gold target discussed in [23][1]. It coincides within the 3.2% systematic error with the normalization factor $R = 0.94 \pm 0.1 \pm 0.32$, which was obtained in [23] for the $0.7–6\%L_R$ gold target in the region $450 < \omega < 500$ MeV[2].

3.1.2. Case $\omega = 0$. In the other limiting case the performance of numerical integration in (36) gets the following results for the relative Coulomb correction $-\delta_{\mathrm{CC}}\left[\langle dI/d\omega\rangle\right]$ and the ratio $R(\omega)|_{\omega=0}$ (Table 3) at thicknesses of experimental gold targets $L = 0.7–6\%L_R$ [23]. Here $L_R \approx 0.33$ cm is the radiation length of the target material $(Z = 79)$

$$L_R = \frac{4Z^2 e^6 n_0}{m^2} \ln\left(183 Z^{1/3}\right).\tag{42}$$

Table 3. **The relative correction** $\delta_{\mathrm{CC}}\left[\langle dI/d\omega\rangle\right]$ **for** $Z = 79$ **and** $\omega = 0$

L, cm	$-\delta_{\mathrm{CC}}\left[\langle dI/d\omega\rangle\right]$	$R_{\mathrm{CC}}\left[\langle dI/d\omega\rangle\right]$
$0.007\,L_R$	0.039	0.961
$0.060\,L_R$	0.018	0.982

3.1.3. Case $\omega_{\mathrm{cr}} > \omega$. When $\omega_{\mathrm{cr}} > \omega > 0$, it is obvious from general considerations that

$$R_{\mathrm{CC}}(\omega)|_{\omega > \omega_{\mathrm{cr}}} \leqslant R_{\mathrm{CC}}(\omega)|_{\omega_{\mathrm{cr}} > \omega} \leqslant R_{\mathrm{CC}}(\omega)|_{\omega=0}.\tag{43}$$

From Table 3 and (43) it follows that the calculation results for $\langle dI/d\omega\rangle$ cannot be obtained from the Born approximation results by multiplying them by the normalization constant, which is independent of the frequency ω and target thickness L.

However, considering a nearly 3.2% systematic error of the experimental data [23] in the range $500 > \omega > 30$ MeV, it is clear why multiplication by the normalization factor helped the authors of [9, 23] to get reasonable agreement of the Born calculation results with the experimental data.

---

[1]The use of approximate Molière's result (28) or (31) for θ_a would give the value $R(\omega)|_{\omega \gg \omega_{\mathrm{cr}}} = 0.900$ in the discussed case.

[2]Migdal used a Gaussian approximation for multiple scattering. This underestimates the probability of large-angle scatters. These occasional large angle scatters would produce some suppression for $\omega > \omega_{\mathrm{cr}}$, where Migdal predicts no suppression and where the authors of [23] determine the normalization [24].

In the conditions of the experiment [23–25] it is permissible to draw conclusions about the size of the normalization factor based on the corrections to the Bethe–Heitler spectrum in the frequency range approximately from 244 to 500 MeV (25 GeV beam and $0.7\% L_R$ gold target). However, in this case some caution is advisable, since 244 to 500 MeV is a rather narrow range. Therefore, let us consider also the second limiting case in order to obtain some interpolation values for $R_{CC}(\omega)|_{\omega_{cr}>\omega}$ from Tables 2 and 3 (Table 4).

Table 4. **The interpolation values of the ratio $R_{CC}(\omega, L)$ for $\omega < \omega_{cr}$, $Z = 79$, and $\beta = 1$**

L, cm	$R_{CC}|_{\omega>\omega_{cr}} \leqslant R_{CC}|_{\omega_{cr}>\omega} \leqslant R_{CC}|_{\omega=0}$	$\bar{R}_{CC}(\omega)|_{\omega<\omega_{cr}}$
$0.007 L_R$	$0.920 \leqslant R_{CC}(\omega)|_{\omega<\omega_{cr}} \leqslant 0.961$	0.940
$0.060 L_R$	$0.920 \leqslant R_{CC}(\omega)|_{\omega<\omega_{cr}} \leqslant 0.982$	0.951

So for $0.007 L_R$ to $0.060 L_R$ gold targets, the averaged value of the ratio $R_{CC}(\omega, L)|_{\omega<\omega_{cr}}$ is approximately 0.945 ± 0.008, which coincides within the experimental error with the normalization factor value $0.94 \pm 0.01 \pm 0.032$ introduced in [23] for obtaining agreement of the calculations performed in the Born approximation with experiment. The obtained result means that the normalization is not required for spectral density of radiation $\langle dI(\omega)/d\omega \rangle$ calculated on the basis of the refined screening angle.

We will now obtain the analytical expressions and numerical estimations for the Coulomb corrections to the function $\nu(\eta) = 2\pi \int \sigma_0(\boldsymbol{\theta})[1 - J_0(\eta\boldsymbol{\theta})]\boldsymbol{\theta} \, d\boldsymbol{\theta}$ (5) and the complex potential $U(\eta) = -\omega\lambda^2/2 - in_0\nu(\eta)$ (34).

For the first quantity, using (26), we obtain

$$\Delta_{CC}[\nu(\eta)] \equiv \nu(\eta) - \nu^B(\eta) = -4\pi\eta^2 \left(\frac{Z\alpha}{\beta p}\right)^2 \Delta_{CC}[\ln(\theta_a')] = -4\pi\eta^2 \left(\frac{Z\alpha}{\beta p}\right)^2 f(\xi). \quad (44)$$

The Coulomb correction to the potential (10) reads

$$\Delta_{CC}[U(\eta)] \equiv U(\eta) - U^B(\eta) = -4\pi in_0\eta^2 \left(\frac{Z\alpha}{\beta p}\right)^2 f(\xi). \quad (45)$$

Now we obtain the corresponding relative Coulomb corrections. Using (5), we get

$$\delta_{CC}[U(\eta)] \equiv \frac{\Delta_{CC}[U(\eta)]}{U^B(\eta)} = \frac{\Delta_{CC}[\nu(\eta)]}{\nu^B(\eta)} \equiv \delta_{CC}[\nu(\eta)]. \quad (46)$$

Then (26), (27), and (44) give

$$\delta_{CC}[\nu(\eta)] = \frac{f(Z\alpha/\beta)}{\ln\eta + \ln(\theta_a^B) - \ln 2 + C_E - 0.5} = -\frac{f(Z\alpha/\beta)}{0.615 - \ln(1.2\alpha Z^{1/3}) - \ln\eta}. \quad (47)$$

We see from (47) and (40) that

$$\delta_{CC}[\nu(\eta)] = \delta_{CC}[U(\eta)] < \delta_{CC}\left[\left\langle\frac{dI}{d\omega}\right\rangle\right], \quad (48)$$

and we can estimate the $\delta_{CC}[\nu(\eta)]$ values using (47) for $\eta \ll 1$. Their numerical values are presented in Table 5.

Table 5. **The relative Coulomb corrections $\delta_{\mathrm{CC}}\big[\nu(\eta)\big]$ and $\delta_{\mathrm{CC}}\big[U(\eta)\big]$ for the gold, lead, and uranium targets**

Target	Z	$a \leqslant \eta \leqslant b$	$-\delta_{\mathrm{CC}}\big[\nu(\eta)\big] = -\delta_{\mathrm{CC}}\big[U(\eta)\big],\%$
Au	79	$0.01 \leqslant \eta \leqslant 0.1$	$3.7 \leqslant -\delta_{\mathrm{CC}}\big[\nu(\eta)\big] \leqslant 5.0$
Pb	82	$0.01 \leqslant \eta \leqslant 0.1$	$3.9 \leqslant -\delta_{\mathrm{CC}}\big[\nu(\eta)\big] \leqslant 5.3$
U	92	$0.01 \leqslant \eta \leqslant 0.1$	$5.5 \leqslant -\delta_{\mathrm{CC}}\big[\nu(\eta)\big] \leqslant 8.0$

Thus, for instance, $-\delta_{\mathrm{CC}}[\nu(\eta)] = -\delta_{\mathrm{CC}}[U(\eta)] \sim 4.3 < -\delta_{\mathrm{CC}}[\langle dI/d\omega\rangle] \sim 8.0\%$ for $Z = 79$ (Au).

Let us consider the spectral bremsstrahlung intensity (6) in the form proposed by Migdal:

$$\left\langle \frac{dI}{d\omega} \right\rangle = \Phi(s) \left(\frac{dI}{d\omega}\right)_0, \tag{49}$$

where $(dI/d\omega)_0$ is the spectral bremsstrahlung rate without accounting for the multiple scattering effects in the radiation,

$$\left(\frac{dI}{d\omega}\right)_0 = \frac{2e^2}{3\pi}\gamma^2 q\, L, \tag{50}$$

$$q = \frac{\overline{\vartheta^2}}{L}. \tag{51}$$

The function $\Phi(s)$ in (49) accounts for the multiple scattering influence on the bremsstrahlung rate,

$$\Phi(s) = 24s^2 \left[\int_0^\infty dx\, \mathrm{e}^{-2sx}\coth(\mathrm{x}) \sin(2\mathrm{sx}) - \frac{\pi}{4}\right], \tag{52}$$

$$s^2 = \frac{\lambda^2}{\overline{\vartheta^2}}. \tag{53}$$

It has simple asymptotes at the small and large values of the argument:

$$\Phi(s) \rightarrow \begin{cases} 6s, & s \rightarrow 0, \\ 1, & s \rightarrow \infty, \end{cases} \tag{54}$$

$$s = \frac{1}{4\gamma^2}\sqrt{\frac{\omega}{q}}. \tag{55}$$

For $s \ll 1$, the suppression is large, and $\Phi(s) \approx 6s$. The intensity of radiation in this case is much less than the corresponding result of Bethe and Heitler. If $s \geqslant 1$ (i.e., $\omega \geqslant \omega_{\mathrm{cr}}$), the function $\Phi(s)$ is close to a unit, and the following approximation is valid [13]:

$$\Phi(s) \approx 1 - 0.012/s^4. \tag{56}$$

The formula (49) is obtained with the logarithmic accuracy. At $s \gg 1$, (49) coincides to the logarithmic accuracy with the Bethe–Heitler result

$$\left\langle \frac{dI}{d\omega} \right\rangle_{\mathrm{BH}} = \frac{L}{L_R}\left[1 + \frac{1}{12\ln\left(183 Z^{-1/3}\right)}\right]. \tag{57}$$

If $s \ll 1$, we have the suppression of the spectral density of radiation in comparison with (57).

Now we obtain analytical and numerical results for the Coulomb corrections to these quantities. In order to derive an analytical expression for the Coulomb correction to the Born spectral bremsstrahlung rate $(dI/d\omega)_0$, we first write

$$\Delta_{\mathrm{CC}}\left[\left(\frac{dI}{d\omega}\right)_0\right] \equiv \left(\frac{dI}{d\omega}\right)_0 - \left(\frac{dI}{d\omega}\right)_0^B = \frac{2e^2}{3\pi}\gamma^2 L\,\Delta_{\mathrm{CC}}[q], \tag{58}$$

$$\Delta_{\mathrm{CC}}[q] \equiv q - q^B = \frac{1}{L}\,\Delta_{\mathrm{CC}}\left[\overline{\vartheta^2}\right]. \tag{59}$$

Accounting for $\overline{\vartheta^2} = \theta_c^2 B$ (21), we get

$$\Delta_{\mathrm{CC}}\left[\overline{\vartheta^2}\right] \equiv \overline{\vartheta^2} - \left(\overline{\vartheta^2}\right)^B = \theta_c^2\,\Delta_{\mathrm{CC}}[B]. \tag{60}$$

Then, using (15) and (17), we arrive at

$$\Delta_{\mathrm{CC}}[b] = -f(\xi) = \left(1 - \frac{1}{B^B}\right)\Delta_{\mathrm{CC}}[B], \tag{61}$$

$$\Delta_{\mathrm{CC}}[B] = \frac{f(\xi)}{1/B^B - 1}. \tag{62}$$

In doing so, (58) becomes

$$\Delta_{\mathrm{CC}}\left[\left(\frac{dI}{d\omega}\right)_0\right] = \frac{2(e\gamma\theta_c)^2}{3\pi\,(1/B^B - 1)}\,f(\xi), \tag{63}$$

and the relative Coulomb correction reads

$$\delta_{\mathrm{CC}}\left[\left(\frac{dI}{d\omega}\right)_0\right] = \delta_{\mathrm{CC}}[q] = \delta_{\mathrm{CC}}\left[\overline{\vartheta^2}\right] = \delta_{\mathrm{CC}}[B] = R_{\mathrm{CC}}\left[\left(\frac{dI}{d\omega}\right)_0\right] - 1 = \frac{f(\xi)}{1 - B^B}. \tag{64}$$

Next, in order to obtain the relative Coulomb correction to the Migdal function $\Phi(s)$, we first derive corresponding correction to the quantity s^2 (53):

$$\Delta_{\mathrm{CC}}\left[s^2\right] = \frac{\omega}{16\gamma^4}\left(\frac{1}{q} - \frac{1}{q^B}\right), \tag{65}$$

$$\delta_{\mathrm{CC}}\left[s^2\right] = \frac{q^B}{q} - 1 = \frac{\left(\overline{\vartheta^2}\right)^B}{\overline{\vartheta^2}} - 1 = \frac{1}{\delta_{\mathrm{CC}}\left[\overline{\vartheta^2}\right] + 1} - 1 = \frac{1}{R_{\mathrm{CC}}\left[(dI/d\omega)_0\right]} - 1. \tag{66}$$

This leads to the following relative Coulomb correction for s (55):

$$\delta_{\mathrm{CC}}\left[s\right] = \frac{1}{\sqrt{\delta_{\mathrm{CC}}\left[\overline{\vartheta^2}\right] + 1}} - 1 = \frac{1}{\sqrt{R_{\mathrm{CC}}\left[(dI/d\omega)_0\right]}} - 1. \tag{67}$$

For the asymptote $\Phi(s) = 6s$ (54), we get

$$\delta_{\mathrm{CC}}\left[\Phi(s)\right] = \delta_{\mathrm{CC}}\left[s\right]. \tag{68}$$

Then, the total relative Coulomb correction to $\langle dI/d\omega \rangle$ in this asymptotic case becomes

$$\delta_{\mathrm{CC}}\left[\left\langle \frac{dI}{d\omega} \right\rangle \right] = \delta_{\mathrm{CC}}\left[\left(\frac{dI}{d\omega} \right)_0 \right] + \delta_{\mathrm{CC}}\left[\Phi(s)\right]. \tag{69}$$

Numerical values of these corrections for some specified values of the Molière parameter B^B are presented in Table 6.

As can be seen from Table 6, the moduli of the Coulomb corrections to the quantities $(dI/d\omega)_0^B$ and $\Phi^B(s)$ decrease from about 9 to 4% and from 5 to 2%, respectively, with an increase in the parameter B^B from a minimum value of 4.5 [30] to a value of 8.46 corresponding to the conditions of experiment [33]; and the modulus of the total relative correction $\delta_{\mathrm{CC}}[\langle dI/d\omega \rangle]$ decreases from approximately 14 to 6%.

Table 6. **Relative Coulomb corrections to the parameters of the Migdal LPM theory, $\delta_{\mathrm{CC}}\left[(dI/d\omega)_0\right]$ (64), $\delta_{\mathrm{CC}}\left[\Phi(s)\right]$ (68), and $\delta_{\mathrm{CC}}\left[\langle dI/d\omega \rangle\right]$ (69), in the regime of strong LPM suppression for $Z = 79$ (Au) and $\beta = 1$**

B^B	$\delta_{\mathrm{CC}}\left[\left(\dfrac{dI}{d\omega} \right)_0 \right]$	$R_{\mathrm{CC}}\left[\left(\dfrac{dI}{d\omega} \right)_0 \right]$	$\delta_{\mathrm{CC}}\left[\Phi(s)\right]$	$\delta_{\mathrm{CC}}\left[\left\langle \dfrac{dI}{d\omega} \right\rangle \right]$	$R_{\mathrm{CC}}\left[\left\langle \dfrac{dI}{d\omega} \right\rangle \right]$
4.50	−0.089	0.911	−0.048	−0.137	0.863
4.90	−0.080	0.920	−0.043	−0.123	0.877
8.46	−0.042	0.958	−0.022	−0.064	0.936

The average value of the ratio $\bar{R}_{\mathrm{CC}} = 0.947 \pm 0.015$ for the gold target is close to the corresponding value $\bar{R}_{\mathrm{CC}} = 0.945 \pm 0.008$ from Table 4. This corresponds to the average size of the relative Coulomb correction -5.4%, which coincides with the size of the normalization correction $(-5.5 \pm 0.2)\%$ for $6\% L_R$ gold target (Table II in [24]).

A comparison of the non-averaged ratio value $R_{\mathrm{CC}}[\langle dI/d\omega \rangle] = 0.936$ from Table 6 with the normalization factor $R \sim 0.94$ would be unjustified, because the regime of strong suppression is not achieved in the analyzed SLAC experiment. For such a comparison, we will carry out now calculation for the regime of small LPM suppression (56).

In order to obtain the relative correction $\delta_{\mathrm{CC}}[\Phi(s)]$ in this regime, we first derive an expression for the Coulomb correction $\Delta_{\mathrm{CC}}[\Phi(s)]$ to the Migdal function $\Phi(s)$:

$$\Delta_{\mathrm{CC}}\left[\Phi(s)\right] = 0.012 \left(\frac{1}{(s^4)^B} - \frac{1}{s^4} \right) = \frac{0.012}{s^4}\,\delta_{\mathrm{CC}}\left[s^4\right], \tag{70}$$

$$\delta_{\mathrm{CC}}\left[s^4\right] = \left(\frac{q^B}{q} \right)^2 - 1 = \left(\frac{\overline{(\vartheta^2)}^B}{\overline{\vartheta^2}} \right)^2 - 1 = \frac{1}{\left(\delta_{\mathrm{CC}}\left[\overline{\vartheta^2}\right] + 1 \right)^2} - 1 =$$
$$= \frac{1}{\left(R_{\mathrm{CC}}\left[(dI/d\omega)_0 \right] \right)^2} - 1. \tag{71}$$

This leads to the following relative Coulomb correction for $\Phi(s)$ (56):

$$\delta_{\mathrm{CC}}\left[\Phi(s)\right] = \frac{0.012}{s^4}\,\delta_{\mathrm{CC}}\left[s^4\right]\,\frac{(s^4)^B}{(s^4)^B - 0.012} = 0.012\,\frac{\delta_{\mathrm{CC}}\left[s^4\right]}{\delta_{\mathrm{CC}}\left[s^4\right] + 1}\,\frac{1}{(s^4)^B - 0.012}. \tag{72}$$

Table 7. **Relative Coulomb corrections to the quantities of the Migdal LPM theory, $\delta_{\mathrm{CC}}\left[(dI/d\omega)_0\right]$ (64), $\delta_{\mathrm{CC}}[\Phi(s)]$ (72), and $\delta_{\mathrm{CC}}[\langle dI/d\omega\rangle]$ (69), in the regime of small LPM suppression for high-Z targets of experiment [24]**

Target	Z	$\delta_{\mathrm{CC}}\left[\left(\dfrac{dI}{d\omega}\right)_0\right]$	$\delta_{\mathrm{CC}}\left[s^4\right]$	$\delta_{\mathrm{CC}}[\Phi(s)]$	$\delta_{\mathrm{CC}}\left[\left\langle\dfrac{dI}{d\omega}\right\rangle\right]$	$R_{\mathrm{CC}}\left[\left\langle\dfrac{dI}{d\omega}\right\rangle\right]$
1. For $\beta = 1$, $B^B = 8.46$, $s = 1.2$
Au	79	-0.0420	-0.0896	-0.0006	-0.0426	0.9574
Pb	82	-0.0445	-0.0953	-0.0006	-0.0451	0.9549
U	92	-0.0529	-0.1149	-0.0007	-0.0536	0.9464
2. For $\beta = 1$, $B^B = 8.46$, $s = 1.3$
Au	79	-0.0420	-0.0896	-0.0004	-0.0424	0.9576
Pb	82	-0.0445	-0.0953	-0.0004	-0.0449	0.9551
U	92	-0.0529	-0.1149	-0.0005	-0.0534	0.9466

Note. For case 1 $\bar{R}_{\mathrm{CC}}[\langle dI/d\omega\rangle] = 0.953 \pm 0.006$; $\bar{\delta}_{\mathrm{CC}}[\langle dI/d\omega\rangle] = (-4.71 \pm 0.58)\%$.
For case 2 $\bar{R}_{\mathrm{CC}}[\langle dI/d\omega\rangle] = 0.953 \pm 0.006$; $\bar{\delta}_{\mathrm{CC}}[\langle dI/d\omega\rangle] = (-4.69 \pm 0.58)\%$.
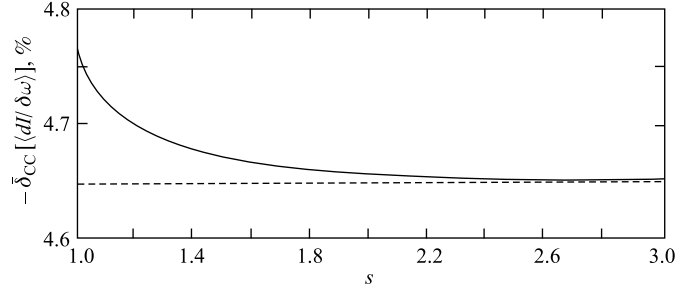
Fig. 1. The s dependence of the corrections $-\bar{\delta}_{\mathrm{CC}}[\langle dI/d\omega\rangle]$ (%) in the entire range $1.0 \leqslant s \leqslant \infty$ of the parameter s

In Table 7 are listed the values of the relative Coulomb corrections to the quantities of (49) in the regime of small suppression (56) for some separate s values ($s = 1.2$ and $s = 1.3$).

Figure 1 demonstrates the s dependence of these corrections $-\bar{\delta}_{\mathrm{CC}}[\langle dI/d\omega\rangle]$ (%) in the entire range $1.0 \leqslant s \leqslant \infty$ of the parameter s, for which the regime of small LPM suppression is valid. Its asymptotic value corresponds to $\bar{\delta}_{\mathrm{CC}}[(dI/d\omega)_0] = (-4.65 \pm 0.45)\%$.

Table 8 presents the values of the corrections $-\delta_{\mathrm{CC}}[\langle dI/d\omega\rangle]$ (%) for some separate target elements and the sampling mean $-\bar{\delta}_{\mathrm{CC}}[\langle dI/d\omega\rangle]$ (%) over the range $1.0 \leqslant s \leqslant \infty$.

Table 8 shows that the Coulomb corrections $\delta_{\mathrm{CC}}[\langle dI/d\omega\rangle] = (-4.50 \pm 0.05)\%$ ($Z = 82$) and $\delta_{\mathrm{CC}}[\langle dI/d\omega\rangle] = (-5.35 \pm 0.06)\%$ ($Z = 92$) coincide within the experimental error with the sizes of the normalization correction values $(-4.5 \pm 0.2)\%$ for $2\%L_R$ lead target and $(-5.6 \pm 0.3)\%$ for $3\%L_R$ uranium target (Table II in [24]), respectively[1].

---

[1]For low-Z targets, the E-146 data showed a disagreement with the Migdal LPM theory predictions. There is a problem of an adequate description of the photon spectra shape for the low-Z targets [24, 25]. Therefore, we will analyze only results for some high-Z targets of the SLAC E-146 experiment.

Table 8. **The dependence of** $-\delta_{\mathrm{CC}}\left[\langle dI/d\omega \rangle\right]$ **values on the parameter** s **in the regime of small LPM suppression for high-Z targets,** $\beta = 1$ **and** $B^B = 8.46$

Target	Z	$s = 1.0$	$s = 1.1$	$s = 1.2$	$s = 1.3$	$s = 1.5$	$s = 2.0$	$s = \infty$
Au	79	0.0432	0.0428	0.0426	0.0424	0.0422	0.0421	0.0420
Pb	82	0.0458	0.0454	0.0451	0.0449	0.0447	0.0446	0.0445
U	92	0.0545	0.0540	0.0536	0.0534	0.0532	0.0530	0.0529
Note. $\delta_{\mathrm{CC}}\left[\langle dI/d\omega \rangle\right] = (-4.50 \pm 0.05)\%$ $(Z = 82)$, $\delta_{\mathrm{CC}}\left[\langle dI/d\omega \rangle\right] = (-5.35 \pm$ $\pm 0.06\%)$ $(Z = 92)$, $\bar{\delta}_{\mathrm{CC}}\left[\langle dI/d\omega \rangle\right] = (-4.70 \pm 0.49)\%$.								

The average value $\bar{\delta}_{\mathrm{CC}}\left[\langle dI/d\omega \rangle\right] = (-4.70 \pm 0.49)\%$ excellently agrees with the weighted average value $(-4.7 \pm 2)\%$ of the normalization correction obtained in [24] for 25 GeV data[1]. We believe that this allows one to understand the origin of the normalization problem for high-Z targets discussed in [23, 24].

3.1.4. Fokker–Planck Approximation Accuracy in the $\omega = 0$ Case. Finally, let us briefly discuss the accuracy of the Fokker–Planck approximation that allows an analytical expression to be derived for the Migdal particle distribution function and entire $\langle dI(\omega)/d\omega \rangle$ range to be rather simply calculated (using numerical calculation of triple integrals).

To this end, we will fix the parameter a in expression (34) in such a way that the results of the exact calculation of $\langle dI(\omega)/d\omega \rangle\big|_{\omega \gg \omega_{\mathrm{cr}}}$ and its calculation in the Fokker–Planck approximation coincide. As a result, we get

$$a = 2\pi \left(\frac{Z\alpha\sigma}{m} \right)^2 \left(\ln \frac{\sigma}{\theta_a} + \frac{7}{12} \right). \tag{73}$$

Now we calculate $\langle dI(\omega)/d\omega \rangle\big|_{\omega=0}$ using the relations (34) and (73) and compare the result with the result obtained using 'realistic' (Molière) expression (26) for $\nu(\eta)$. Then for the ratio

$$R_{\mathrm{FPM}} = \frac{\langle dI(\omega)/d\omega \rangle_{\mathrm{FP}}}{\langle dI(\omega)/d\omega \rangle_M} \tag{74}$$

we get the following values:

$$R_{\mathrm{FPM}}(\omega, L) = \begin{cases} 0.890, & L = 0.007 L_R, \\ 0.872, & L = 0.060 L_R. \end{cases} \tag{75}$$

The values of the corresponding relative corrections

$$\delta_{\mathrm{FPM}}\left[\left\langle \frac{dI}{d\omega} \right\rangle \right] = \frac{\langle dI(\omega)/d\omega \rangle_{\mathrm{FP}} - \langle dI(\omega)/d\omega \rangle_M}{\langle dI(\omega)/d\omega \rangle_M} \tag{76}$$

in percentage are given in Table 9.

It is obvious that the relative difference between the Fokker–Planck approximation and the description based on the Molière theory $\delta_{\mathrm{FPM}}\left[\langle dI/d\omega \rangle\right]$ is about 12%, which is noticeably higher than the 3.2% characteristic systematic experimental error [23].

---

[1]It becomes $(-4.8 \pm 3.5)\%$ for the 8 GeV data if the outlying $6\% L_R$ gold target is excluded from them [24].

Table 9. **The relative correction $\delta_{\mathrm{FPM}}\left[\langle dI/d\omega\rangle\right]$ for $Z = 79$ and $\omega = 0$**

L, cm	$-\delta_{\mathrm{FPM}}\left[\langle dI/d\omega\rangle\right]$	$R_{\mathrm{FPM}}\left[\langle dI/d\omega\rangle\right]$
$0.007L_R$	0.110	0.890
$0.060L_R$	0.128	0.872

Thus, the Fokker–Planck approximation and Gaussian distribution cannot be used for describing the experimental data [23,24] at low frequencies $\omega < 30$ MeV. For their description the application of the Molière multiple scattering theory is advisable.

3.2. Coulomb Corrections in the LPM Effect Theory Analogue for a Thin Target. In [33] it is shown that the region of the emitted photon frequencies $\omega_{\mathrm{cr}} > \omega > 0$ naturally splits into two intervals, $\omega_{\mathrm{cr}} > \omega > \omega_c$ and $\omega_c > \omega > 0$, in the first of which the LPM effect for sufficiently thick targets takes place, and in the second, there is its analogue for thin targets. The quantity ω_c is defined here as $\omega_c = 2E^2/(m^2L)$.

Application of the Molière multiple-scattering theory to the analysis of experimental data [23, 24] for a thin target in the second ω range is based on the use of the expression for the particle distribution function (11) which satisfies the standard Boltzmann transport equation for a thin homogeneous foil, and it differs significantly from the Gaussian particle distribution of the Migdal LPM effect theory.

Besides, it determines another expression for the spectral radiation rate in the context of the coherent radiation theory [33][1], which reads

$$\left\langle \frac{dI}{d\omega} \right\rangle = \int w_M(\vartheta)\frac{dI(\vartheta)}{d\omega}\,d^2\vartheta. \tag{77}$$

Here

$$\frac{dI(\vartheta)}{d\omega} = \frac{2e^2}{\pi}\left[\frac{2\chi^2+1}{\chi\sqrt{\chi^2+1}}\ln\left(\chi+\sqrt{\chi^2+1}\right)-1\right] \tag{78}$$

with $\chi = \gamma\vartheta/2$. The latter expression is valid for consideration of the particle scattering in both amorphous and crystalline medium.

The formula (78) has simple asymptotes at the small and large values of the parameter $\chi = \gamma\vartheta/2$:

$$\frac{dI(\vartheta)}{d\omega} = \frac{2e^2}{3\pi}\left\{ \begin{array}{ll} \gamma^2\vartheta^2, & \gamma\vartheta \ll 1, \\ 3[\ln(\gamma^2\vartheta^2)-1], & \gamma\vartheta \gg 1, \end{array} \right. \tag{79}$$

Replacing ϑ^2 by the average square value of the scattering angle $\overline{\vartheta^2}$ in this formula, we arrive at the following estimates for the average radiation spectral density value:

$$\left\langle \frac{dI}{d\omega} \right\rangle = \frac{2e^2}{3\pi}\left\{ \begin{array}{ll} \gamma^2\overline{\vartheta^2}, & \gamma^2\overline{\vartheta^2} \ll 1, \\ 3[\ln(\gamma^2\overline{\vartheta^2})-1], & \gamma^2\overline{\vartheta^2} \gg 1. \end{array} \right. \tag{80}$$

---

[1]Note that the authors of [33] neglect the influence of the medium polarization [37] on the radiation in this theory. This is admissible in the conditions of the experiment [23,24], where the LPM effect is more important for photon energies above 5 MeV (at 25 GeV beams); and dielectric suppression dominates at significantly lower photon energies.

In the experiment [23, 24], the above frequency intervals correspond roughly to the following ω ranges: $(\omega_{\mathrm{cr}} > \omega > \omega_c) \sim (244 > \omega > 30 \text{ MeV})$ and $(\omega_c > \omega > 0) \sim (30 > \omega > 5 \text{ MeV})$ for 25 GeV electron beam and $0.7{-}6.0\%L_R$ gold target. Whereas in the first area the discrepancy between the LPM theory predictions and data is about 3.2 to 5%, in the second area this discrepancy reaches $\sim 15\%$.

Using the approximate second-order representation of the Molière distribution function (24), (25) for computing the spectral radiation rate (77), the authors of [33] succeeded in bringing theory and $0.7\%L_R$ (25 GeV) data into satisfactory agreement over the ω range 5 to 30 MeV.

This result can be understood by considering the fact that the correction of order of $1/B^B$ to the Gaussian first-order representation of the distribution function $w_M(\vartheta)$ is about 12% for the value used in calculations $B^B = 8.46$ [33].

Let us obtain the relative Coulomb correction to the average value of the spectral density of radiation for two limiting cases (80).

In the first case $\gamma^2\overline{\vartheta^2} \ll 1$, taking into account the equality

$$\delta_{\mathrm{CC}}[\gamma^2\overline{\vartheta^2}] = \delta_{\mathrm{CC}}[\overline{\vartheta^2}], \tag{81}$$

(64), and (80), we get

$$\delta_{\mathrm{CC}}\left[\left\langle \frac{dI}{d\omega} \right\rangle\right] = \delta_{\mathrm{CC}}\left[\left(\frac{dI}{d\omega}\right)_0\right] = \frac{f(\xi)}{1 - B^B}, \tag{82}$$

where $B^B \approx 8.46$ in the conditions of the discussed experiment [33].

In the second case $\gamma^2\overline{\vartheta^2} \gg 1$, we have

$$\Delta_{\mathrm{CC}}\left[\ln\left(\gamma^2\overline{\vartheta^2}\right) - 1\right] = \Delta_{\mathrm{CC}}\left[\ln\left(\overline{\vartheta^2}\right)\right] = \Delta_{\mathrm{CC}}\left[\ln\left(B\right)\right]. \tag{83}$$

For the latter quantity, one can obtain

$$\Delta_{\mathrm{CC}}[\ln(B)] = \Delta_{\mathrm{CC}}[B] + f(Z\alpha) = \delta_{\mathrm{CC}}[B]. \tag{84}$$

The Coulomb correction then becomes

$$\Delta_{\mathrm{CC}}\left[\ln\left(\gamma^2\overline{\vartheta^2}\right) - 1\right] = \frac{\delta_{\mathrm{CC}}[B]}{\left[\ln(\gamma^2\overline{\vartheta^2})^B - 1\right]}. \tag{85}$$

Taking into account (64), we arrive at

$$\delta_{\mathrm{CC}}\left[\left\langle \frac{dI}{d\omega} \right\rangle\right] = \frac{f(\xi)}{\left[\ln(\gamma^2\overline{\vartheta^2})^B - 1\right]\left(1 - B^B\right)}. \tag{86}$$

The numerical values of these corrections are presented in Table 10.

The second asymptote is not reached [33] in the experiment [23, 24]. Therefore, we will now consider another limiting case corresponding to the experimental conditions and taking into account the second term of the Molière distribution function expansion (19).

Table 10. **The relative Coulomb correction** $\delta_{\mathrm{CC}}\left[\langle dI/d\omega\rangle\right]$ **to the asymptotes of the Born spectral radiation rate over the range** $\omega < \omega_c$ **for** $\beta = 1$, $B^B \approx 8.46$, **and** $\left(\gamma^2\overline{\vartheta^2}\right)^B \approx 7.61$ **[33]**

Target	Z	$\gamma^2\overline{\vartheta^2}$	$-\delta_{\mathrm{CC}}\left[\langle dI/d\omega\rangle\right]$	R_{CC}
Au	79	$\gamma^2\overline{\vartheta^2} \ll 1$	0.042	0.958
Au	79	$\gamma^2\overline{\vartheta^2} \gg 1$	0.040	0.960

Substituting the second-order expression (24) for the distribution function into (77) and integrating its second term (25), we can arrive at the following expression for the electron radiation spectrum at $\mu^2 = \gamma^2\overline{\vartheta^2} \gg 1$ [33]:

$$\left\langle \frac{dI}{d\omega}\right\rangle = \frac{2e^2}{\pi}\left\{\ln\left(\mu^2\right) - C_E\left(1 + \frac{2}{\mu^2}\right) + \frac{2}{\mu^2} + \frac{C_E}{B} - 1\right\}. \tag{87}$$

In order to obtain the Coulomb correction to the Born spectral radiation rate from (87), we first calculate its numerical value at $(\mu^2)^B \approx 7.61$ and $B^B \approx 8.46$, and we get $\langle dI/d\omega\rangle^B = 0.00542$. The Bethe–Heitler formula in the Born approximation becomes $\langle dI/d\omega\rangle^B_{\mathrm{BH}} = 0.00954$.

Then, we calculate the numerical values of B and μ^2 parameters including the Coulomb corrections. From

$$\Delta_{\mathrm{CC}}[B] = \frac{f(\xi)}{1/B^B - 1} = -0.355, \tag{88}$$

we obtain $B = 8.105$ for $Z = 79$ and $B^B \approx 8.46$. The equality

$$\Delta_{\mathrm{CC}}\left[\ln\mu^2\right] = \Delta_{\mathrm{CC}}\left[\ln B\right] = \Delta_{\mathrm{CC}}[B] + f(\xi) = \delta_{\mathrm{CC}}[B] = -0.042 \tag{89}$$

gets $\ln\mu^2 = 1.987$ and $\mu^2 = 7.295$. Substituting these values into (87), we have $\langle dI/d\omega\rangle = 0.00531$. The relative Coulomb corrections to these parameters are presented in Table 11. These corrections are not large. Their sizes are between two and four percent, i.e., of the order of the experimental error.

Table 11. **The relative Coulomb corrections in the analogue of the LPM effect theory for** $0.07L_R$ **gold target,** $\omega < \omega_c$, **and** $\beta = 1$

$\delta_{\mathrm{CC}}[B]$	$\delta_{\mathrm{CC}}\left[\ln\mu^2\right]$	$\delta_{\mathrm{CC}}\left[(dI/d\omega)_0\right]$	$\delta_{\mathrm{CC}}\left[\langle dI/d\omega\rangle\right]$	$\delta_{\mathrm{CC}}\left[\Phi(s)\right]$
-0.042	-0.021	-0.042	-0.020	-0.021

Accounting for the relative Coulomb correction to the Bethe–Heitler spectrum of bremsstrahlung, we find $(dI/d\omega)_{\mathrm{BH}} = 0.00916$. So we get

$$\left\langle \frac{dI}{d\omega}\right\rangle = 0.580\left(\frac{dI}{d\omega}\right)_{\mathrm{BH}}. \tag{90}$$

This leads to the value of the spectral radiation rate in terms of $dN/[d(\log\omega)]\,1/L_R$, where N is the number of events per photon energy bin per incident electron, $dN/[d(\log\omega)/L_R] = 0.118\cdot0.580 = 0.068$, which agrees very well with the experimental result over the frequency
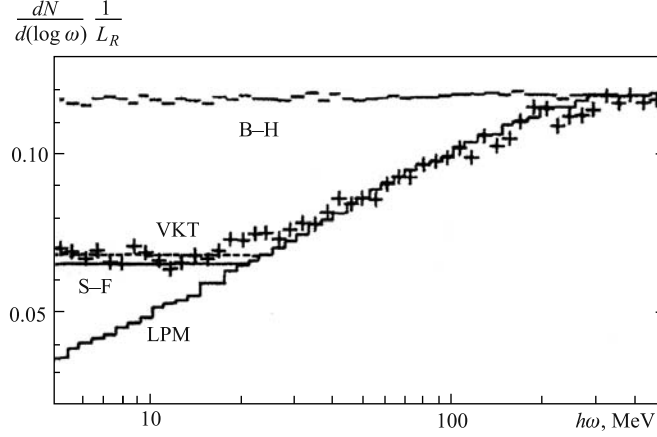
Fig. 2. Measurement of the LPM effect over the range $30 < \omega < 500$ MeV and its analogue in the range $5 < \omega < 30$ MeV for the $0.7\% L_R$ gold target and 25 GeV electron beam. The signs «+» denote the experimental data; the histograms B–H and LPM give the Bethe–Heitler and the LPM Monte Carlo predictions [23]. The solid and dashed lines (S–F and VKT) over the range $\omega < 30$ MeV are the results of calculations without [33] and with the obtained Coulomb corrections

range $\omega < 30$ MeV for 25 GeV electron beam and $0.7\% L_R$ gold target. This result additionally improves the agreement between the theory and experiment (see Fig. 2). It is close to the Zakharov result [10] and coincides with the result of Blancenbeckler and Drell obtained in the eikonal approximation, which excellently agrees with $0.7\% L_R$ (25 GeV) data for $\omega > 5$ MeV (see Figs. 12, *a* in [24] and 20, *a* in [25]).

4. SUMMARY AND CONCLUSIONS

• Within the theory of LPM effect for finite-size targets, we calculated the Coulomb corrections to the Born bremsstrahlung rate $\langle dI(\omega)/d\omega \rangle^B$ and estimated the ratio $\langle dI(\omega)/d\omega \rangle / \langle dI(\omega)/d\omega \rangle^B = R(\omega, L)$ for gold target based on results of the revised Molière multiple scattering theory for the Coulomb corrections to the screening angle.

• We demonstrated that the $R(\omega, L)$ value is close to the normalization constant R value for $0.7-6\% L_R$ (25 GeV) data over the ω range 30 to 500 MeV from [9, 23]; however, the latter ignores the dependence of the ratio on ω and L.

• We have obtained the analytical and numerical results for the Coulomb corrections to the function $\nu(\eta) = 2\pi \int \sigma_0(\boldsymbol{\theta})[1 - J_0(\eta\theta)]\boldsymbol{\theta}\, d\boldsymbol{\theta}$ and complex potential $U(\eta) = -\omega\lambda^2/2 - i\, n_0\nu(\eta)$ and showed that $-\delta_{\mathrm{CC}}[\nu(\eta)] = -\delta_{\mathrm{CC}}[U(\eta)] \sim 4.3\% < -\delta_{\mathrm{CC}}[\langle dI/d\omega \rangle] \sim 8.0\%$ for $Z = 79$ ($\beta = 1$).

• Additionally, we found Coulomb corrections to the quantities of the Migdal LPM theory and some important parameters of the Molière multiple scattering theory, i.e., $\Delta_{\mathrm{CC}}[(dI/d\omega)_0]$, $\Delta_{\mathrm{CC}}[q]$, $\Delta_{\mathrm{CC}}[s^2]$, $\Delta_{\mathrm{CC}}[s^4]$, $\Delta_{\mathrm{CC}}[\Phi(s)]$, $\Delta_{\mathrm{CC}}[\langle dI/d\omega \rangle]$, as well as $\Delta_{\mathrm{CC}}[b]$, $\Delta_{\mathrm{CC}}[B]$, $\Delta_{\mathrm{CC}}[\ln B]$, $\Delta_{\mathrm{CC}}\left[\overline{\vartheta^2}\right]$, and $\Delta_{\mathrm{CC}}\left[\ln\left(\overline{\vartheta^2}\right)\right]$.

• We also calculated relative Coulomb corrections $\delta_{\mathrm{CC}}[(dI/d\omega)_0] = \delta_{\mathrm{CC}}[q] = \delta_{\mathrm{CC}}\left[\overline{\vartheta^2}\right] = \delta_{\mathrm{CC}}[B]$, $\delta_{\mathrm{CC}}[\Phi(s)] = \delta_{\mathrm{CC}}[s]$, and $\delta_{\mathrm{CC}}[\langle dI/d\omega \rangle]$ in the regime of strong LPM suppression for

$Z = 79$ ($\beta = 1$) and showed that the latter correction $\delta_{\text{CC}}\left[\langle dI/d\omega \rangle\right]$ comprises the order of -14% at minimum B^B value 4.5.

• We demonstrated that the average size of the relative Coulomb correction -5.4% coincides with the size of normalization correction $(-5.5 \pm 0.2)\%$ for $6\% L_R$ gold target obtained in the experiment [24].

• We have performed analogous calculations for the regime of small LPM suppression over the entire range $1 \leqslant s \leqslant \infty$. We found that the values of the Coulomb corrections $\delta_{\text{CC}}\left[\langle dI/d\omega \rangle\right] = (-4.50 \pm 0.05)\%$ ($Z = 82$) and $\delta_{\text{CC}}\left[\langle dI/d\omega \rangle\right] = (-5.35 \pm 0.06)\%$ ($Z = 92$) coincide with the mean normalization correction $(-4.5 \pm 0.2)\%$ for $2\% L_R$ lead target and $(-5.6 \pm 0.3)\%$ for $3\% L_R$ uranium target, respectively, within the experimental error.

• The average $\bar{\delta}_{\text{CC}}\left[\langle dI/d\omega \rangle\right] = (-4.70 \pm 0.49)\%$ excellently agrees in the regime of small LPM suppression with the weighted average $(-4.7 \pm 2)\%$ of the normalization correction obtained for 25 GeV data in the experiment [24].

• Thus, we managed to show that the discussed discrepancy between theory and experiment can be explained on the basis of the obtained Coulomb corrections to the Born bremsstrahlung rate within the Migdal LPM effect theory.

• This means that applying the revised multiple scattering theory by Molière allows one to avoid multiplying theoretical results by the above normalization factor and leads to agreement between the Migdal LPM effect theory and experimental data [23, 24] for sufficiently thick high-Z targets over the range $20 < \omega < 500$ MeV.

• We evaluated the accuracy of the Fokker–Planck approach and the Gaussian first-order representation of the distribution function $w_0(\boldsymbol{\vartheta})$ in the limiting case $\omega = 0$ and showed the need of accounting for the second-order correction of the order of $1/B^B \sim 12\%$ for $w(\boldsymbol{\vartheta})$ to eliminate the discrepancy between the theory and experiment over the frequency range $5 < \omega < 30$ MeV for 25 GeV and $0.7\% L_R$ gold target data of the experiment [23, 24].

• Finally, we found the numerical values of the relative corrections $\delta_{\text{CC}}\left[(dI/d\omega)_0\right]$, $\delta_{\text{CC}}\left[\Phi(s)\right]$, and $\delta_{\text{CC}}\left[\langle dI/d\omega \rangle\right]$ in the LPM effect theory analogue for a thin target over the range $5 < \omega < 30$ and demonstrated that these corrections additionally improve the agreement between the theory [32, 33] and experiment [23, 24].

REFERENCES

1. *Landau L. D., Pomeranchuk I. Ya.* The Limits of Applicability of the Theory of Bremsstrahlung by Electrons and of the Creation of Pairs at Large Energies // Dokl. Akad. Nauk SSSR. 1953. V. 92. P. 535;
Landau L. D., Pomeranchuk I. Ya. Electron-cascade processes at ultra-high energies // Ibid. P. 735.

2. *Migdal A. B.* The Influence of the Multiple Scattering on the Bremsstrahlung at High Energies // Dokl. Akad. Nauk SSSR. 1954. V. 96. P. 49.

3. *Migdal A. B.* Bremsstrahlung and Pair Production in Condensed Media at High Energies // Phys. Rev. 1956. V. 103. P. 1811.

4. *Goldman I. I.* Bremsstrahlung at the Boundary of a Medium with Account of Multiple Scattering // JETP. 1960. V. 38. P. 1866.

5. *Baier V. N., Katkov V. M., Strakhovenko V. M.* Radiation at Collision of Relativistic Particles in Media in the Presence of External Field // JETP. 1988. V. 67. P. 70;
   Baier V. N., Katkov V. M. The Theory of the Landau–Pomeranchuk–Migdal Effect // Phys. Rev. D. 1998. V. 57. P. 3146.

6. *Baier V. N., Katkov V. M., Fadin V. S.* Radiation from Relativistic Electrons. M.: Atomizdat, 1973 (in Russian);
   Baier V. N., Katkov V. M., Strakhovenko V. M. Electromagnetic Processes at High Energies in Oriented Single Crystals. Singapore: World Sci. Publ. Co, 1997.

7. *Laskin N. V., Mazmanishvili A. S., Shul'ga N. F.* Continual Method in the Problem of Multiple-Scattering Effect on Radiation by High-Energy Particle in Amorphous Media and Crystals // Dokl. Akad. Nauk SSSR. 1984. V. 277. P. 850;
   Laskin N. V., Mazmanishvili A. S., Shul'ga N. F. A Method of Path Integration and Landau–Pomeranchuk Effect of Suppression of Fast-Particle Radiation in Matter // Phys. Lett. A. 1985. V. 112. P. 240;
   Akhiezer A. I., Laskin N. V., Shul'ga N. F. Method of Functional Integration in Quantum Theory of Radiation by Fast Charged Particles in Matter // Dokl. Akad. Nauk SSSR. 1987. V. 295. P. 1363.

8. *Zakharov B. G.* Fully Quantum Treatment of the Landau–Pomeranchuk–Migdal Effect in QED and QCD // JETP Lett. 1996. V. 63. P. 952;
   Zakharov B. G. Light-Cone Path Integral Approach to the Landau–Pomeranchuk–Migdal Effect // Phys. At. Nucl. 1998. V. 61. P. 838.

9. *Zakharov B. G.* Landau–Pomeranchuk–Migdal Effect for Finite-Size Targets // JETP Lett. 1996. V. 64. P. 781.

10. *Zakharov B. G.* Light-Cone Path Integral Approach to the Landau–Pomeranchuk–Migdal Effect and the SLAC Data on Bremsstrahlung from High-Energy Electrons // Yad. Fiz. 1999. V. 62. P. 1075.

11. *Blancenbeckler R., Drell S. D.* The Landau–Pomeranchuk–Migdal Effect for Finite Targets // Phys. Rev. D. 1996. V. 53. P. 6265;
    Blancenbeckler R. Structured Targets and the Landau–Pomeranchuk–Migdal Effect // Phys. Rev. D. 1997. V. 55. P. 190.

12. *Blancenbeckler R.* Multiple Scattering and Functional Integrals // Ibid. P. 2441.

13. *Shul'ga N. F., Fomin S. P.* Suppression of Radiation in an Amorphous Medium and in a Crystal // JETP Lett. 1978. V. 27. P. 117;
    Shul'ga N. F., Fomin S.P. Theoretical and Experimental Investagations of the Landau–Pomeranchuk–Migdal Effect in Amorphous and Crystalline Matter // Probl. At. Sci. Technol. 2003. No. 2. P. 11;
    Shul'ga N. F. Advances in Coherent Bremsstrahlung and LPM-Effect Studies // Intern. J. Mod. Phys. A. 2010. V. 25. P. 9.

14. *Gerhardt L., Klein S. R.* Electron and Photon Interactions in the Regime of Strong LPM Suppression // Phys. Rev. D. 2010. V. 82. P. 074017.

15. *Abbasi R. et al. (IceCube Collab.).* First Observation of PeV-energy Neutrinos with IceCube // Phys. Rev. Lett. 2013. V. 111. P. 021103;
    Klein S. R. Radiodetection of Neutrinos // Nucl. Phys. B. Proc. Suppl. 2012. V. 229–232. P. 284.

16. *Van Goethem M. J. et al.* Suppression of Soft Nuclear Bremsstrahlung in Proton–Nucleus Collisions // Phys. Rev. Lett. 2002. V. 88. P. 122302.

17. *Sørensen A. H.* On the Suppression of the Gluon Radiation for Quark Jets Penetrating a Dense Quark Gas // Z. Phys. C. 1992. V. 53. P. 595;

Brodsky S. J., Hoyer P. A Bound on the Energy Loss of Partons in Nuclei // Phys. Lett. B. 1993. V. 298. P. 165;

Kopeliovich B. Z., Tarasov A. V., Schafer A. Bremsstrahlung of a Quark Propagating through a Nucleus // Phys. Rev. C. 1999. V. 59. P. 1609.

18. *Gyulassy M., Wang X. N.* Multiple Collisions and Induced Gluon Bremsstrahlung in QCD // Nucl. Phys. B. 1994. V. 420. P. 583;
    Gyulassy M., Levai P., Vitev I. Reaction Operator Approach to Non-Abelian Energy Loss // Nucl. Phys. B. 2001. V. 594. P. 371.

19. *Baier R. et al.* Induced Gluon Radiation in a QCD Medium // Phys. Lett. B. 1995. V. 345. P. 277;
    Baier R. et al. The Landau–Pomeranchuk–Migdal Effect in QED // Nucl. Phys. B. 1996. V. 478. P. 577;
    Baier R. et al. Medium-Induced Radiative Energy Loss; Equivalence between the BDMPS and Zakharov Formalisms // Nucl. Phys. B. 1998. V. 531. P. 403.

20. *Baier V. N., Katkov V. M.* Coherent and Incoherent Radiation from High-Energy Electron and the LPM Effect in Oriented Single Crystal // Phys. Lett. A. 2006. V. 353. P. 91.

21. *Raffelt G., Seckel D.* Multiple-Scattering Suppression of Bremsstrahlung Emission of Neutrinos and Axions in Supernovae // Phys. Rev. Lett. 1991. V. 67. P. 2605;
    Pethick C. J., Thorsson V. Neutrino Pair Bremsstrahlung in Neutron Star Crusts: A Reappraisal // Phys. Rev. Lett. 1994. V. 72. P. 1964.

22. *Baier R. et al.* Radiative Energy Loss of High-Energy Quarks and Gluons in a Finite Volume Quark Gluon Plasma // Nucl. Phys. B. 1997. V. 483. P. 291;
    Peignè S., Smilga A. V. Energy Losses in Relativistic Plasmas: QCD versus QED // Phys. Usp. 2009. V. 179. P. 697.

23. *Anthony P. L. et al.* An Accurate Measurement of the Landau–Pomeranchuk–Migdal Effect // Phys. Rev. Lett. 1995. V. 75. P. 1949;
    Anthony P. L. et al. Measurement of Dielectric Suppression of Bremsstrahlung // Phys. Rev. Lett. 1996. V. 76. P. 3550.

24. *Anthony P. L. et al.* Bremsstrahlung Suppression Due to the LPM and Dielectric Effects in a Variety of Targets // Phys. Rev. D. 1997. V. 56. P. 1373.

25. *Klein S. R.* Suppression of Bremsstrahlung and Pair Production Due to Environmental Factors // Rev. Mod. Phys. 1999. V. 71. P. 1501.

26. *Hansen H. D. et al.* Landau–Pomeranchuk–Migdal Effect for Multihundred GeV Electrons // Phys. Rev. D. 2004. V. 69. P. 032001.

27. *Andersen J. U. et al.* (*CERN-NA63 Collab.*). Electromagnetic Processes in Strong Crystalline Fields // Phys. Lett. B. 2009. V. 672. P. 323.

28. *Tarasov A. V., Voskresenskaya O. O.* An Improvement of the Molière–Fano Multiple Scattering Theory // Alexander Vasilievich Tarasov: To the 70th Birth Anniversary. Dubna: JINR, 2012. P. 276;
    Tarasov A. V., Voskresenskaya O. O. Molière's Multiple Scattering Theory Revisited. arXiv:1204.3675 [hep-ph].

29. *Kuraev E. A., Voskresenskaya O. O., Tarasov A. V.* Coulomb Correction to the Screening Angle of the Molière Multiple Scattering Theory. JINR Preprint E2-2012-135. Dubna, 2012. 14 p.; arXiv:1211.6961 [hep-ph].

30. *Molière G.* Theorie der Streuung schneller geladener Teilchen: I. Einzelstreuung am abgeschirmten Coulomb-Feld // Z. Naturforsch. 1947. V. 2a. P. 133;
    Molière G. Theorie der Streuung schneller geladener Teilchen: II. Mehrfach- und Vielfachstreuung // Z. Naturforsch. 1948. V. 3a. P. 78.

31. *Bethe H. A.* Molière's Theory of Multiple Scattering // Phys. Rev. 1953. V. 89. P. 256.

32. *Shul'ga N. F., Fomin S. P.* On the Experimental Verification of the Landau–Pomeranchuk–Migdal Effect // JETP Lett. 1996. V. 63. P. 873.

33. *Shul'ga N. F., Fomin S. P.* Effect of Multiple Scattering on the Emission of Ultrarelativistic Electrons in a Thin Layer of Matter // JETP Lett. 1998. V. 113. P. 58.

34. *Feynman R. P., Hibbs A. R.* Quantum Mechanics and Path Integrals. New York: McGrav-Hill, 1965.

35. *Voskresenskaya O. O. et al.* Theory of the Landau–Pomeranchuk Effect for Finite-Size Targets. JINR Preprint P2-97-308. Dubna, 1997. 8 p.;
    Tarasov A. V., Torosyan H. T., Voskresenskaya O. O. A Quasiclassical Approximation in the Theory of the Landau–Pomeranchuk Effect. arXiv:1203.4853 [hep-ph].

36. *Scott W. T.* The Theory of Small-Angle Multiple Scattering of Fast Charged Particles // Rev. Mod. Phys. 1963. V. 35. P. 231.

37. *Ter-Mikaelian M. L.* Scatter of High-Energy Electrons in Crystals // Zh. Eksp. Teor. Fiz. 1953. V. 25. P. 289;
    Ter-Mikaelian M. L. The Interference Emission of High-Energy Electrons // Ibid. P. 296;
    Ter-Mikaelian M. L. High-Energy Electromagnetic Processes in Condensed Media. New York: Wiley Intersci., 1972.